

**OMTM, Volume 25**

**Supplemental information**

**A flexible, thermostable nanostructured  
lipid carrier platform for RNA vaccine delivery**

**Alana Gerhardt, Emily Voigt, Michelle Archer, Sierra Reed, Elise Larson, Neal Van  
Hoeven, Ryan Kramer, Christopher Fox, and Corey Casper**

Supplemental Information

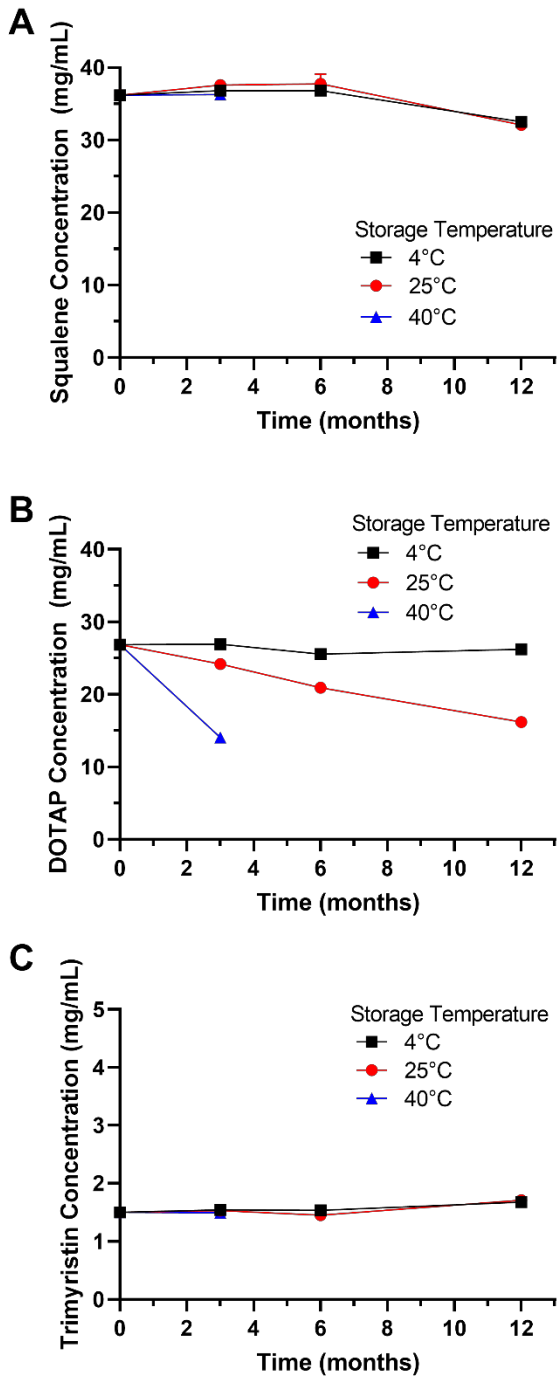


**Figure S1.** Concentrations of NLC components squalene (A), DOTAP (B), and trimyristin (C) by HPLC after long-term storage at 4°C (black), 25°C (red), and 40°C (blue).

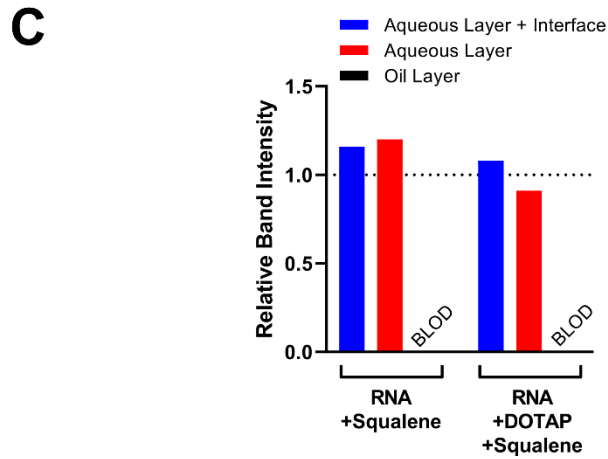
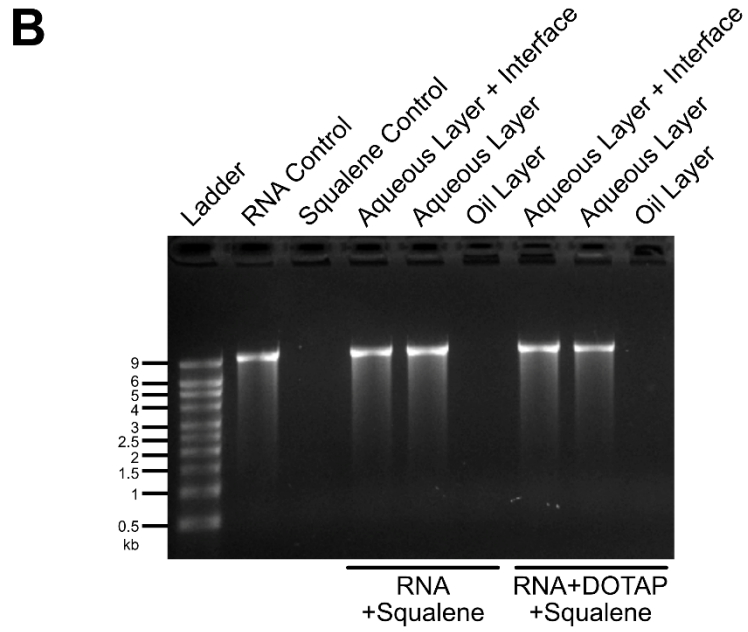
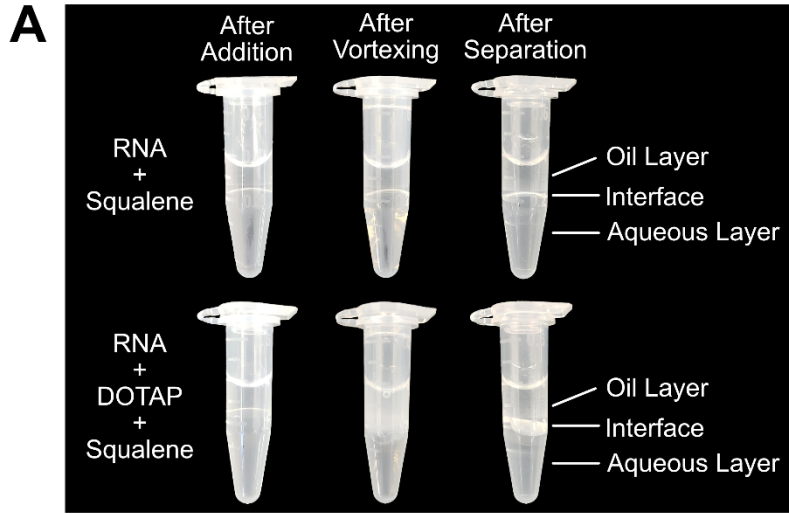


**Figure S2.**

Evaluation of the solubility of RNA in squalene and DOTAP-complexed RNA in squalene. (A) RNA was added to vials of squalene alone (top row) or DOTAP solubilized in squalene (bottom row). Images of the vials were taken immediately after the addition of the RNA component to the oil component (left), after vortexing the vials (middle), and after separation of the phases (right). Complexing of the RNA with DOTAP is observed as an increase in turbidity in the bottom middle image. An interfacial layer of DOTAP-complexed RNA is visible after separation in the bottom right image. (B) After separation, each layer was removed and evaluated by agarose gel electrophoresis to detect RNA. No RNA was detected in the oil layer in the presence or absence of DOTAP. (C) Densitometry analysis of the agarose gel in Panel B. The intensity of the RNA band for each layer is quantified relative to the RNA control lane which was set to have an intensity of 1. RNA in the oil layers was below the limit of detection (BL0D).

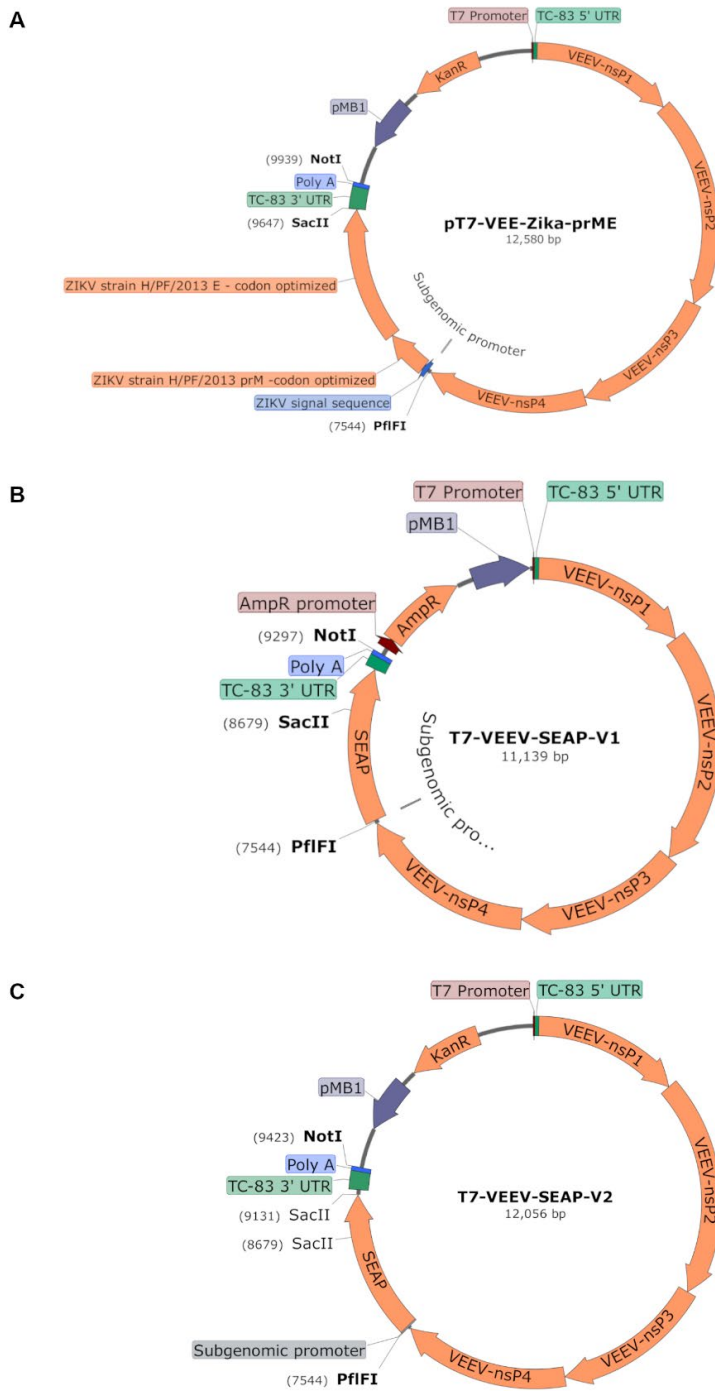


**Figure S3.**

DNA plasmid templates for self-amplifying RNA vaccine constructs. RNA replicons consist of the 5'UTR, non-structural proteins, and 3'UTR sequences of the attenuated TC-83 strain of Venezuelan equine encephalitis virus (VEEV) with Zika virus prM-E genes (A) or the secreted alkaline phosphatase (SEAP) gene (B, C) inserted in place of VEEV structural proteins, as described in the Methods section "saRNA DNA Templates".

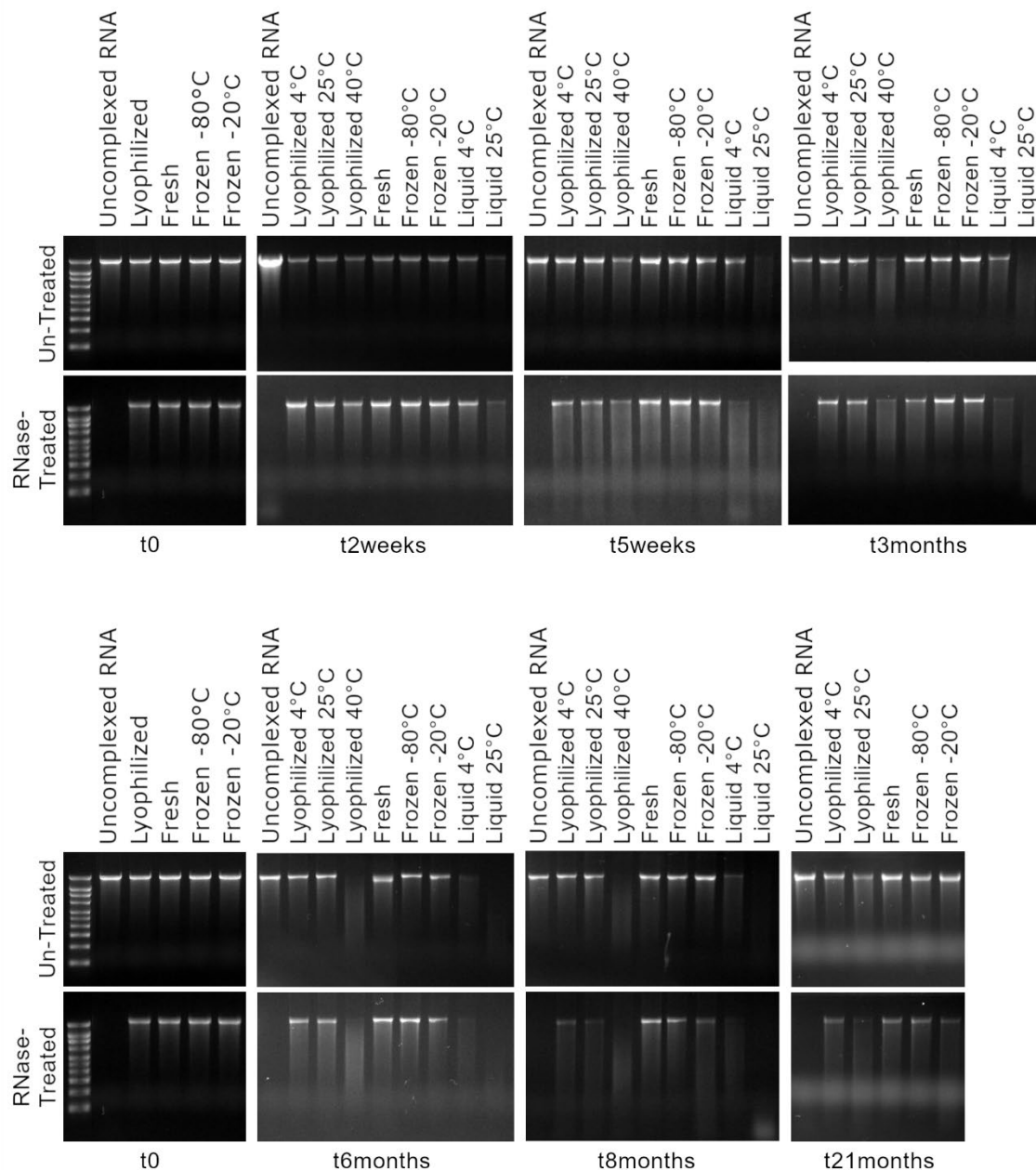


**Figure S4.**

RNA integrity of the stored SEAP NLC/saRNA samples after extraction from the NLC complex (“Un-Treated”) and protection of RNA after RNase treatment and then extraction from the NLC complex (“RNase-Treated”) by agarose gel electrophoresis for each condition at each timepoint. (Note that cropped portions of the gels in this figure appear in Figure 1E and Figure 4C.)

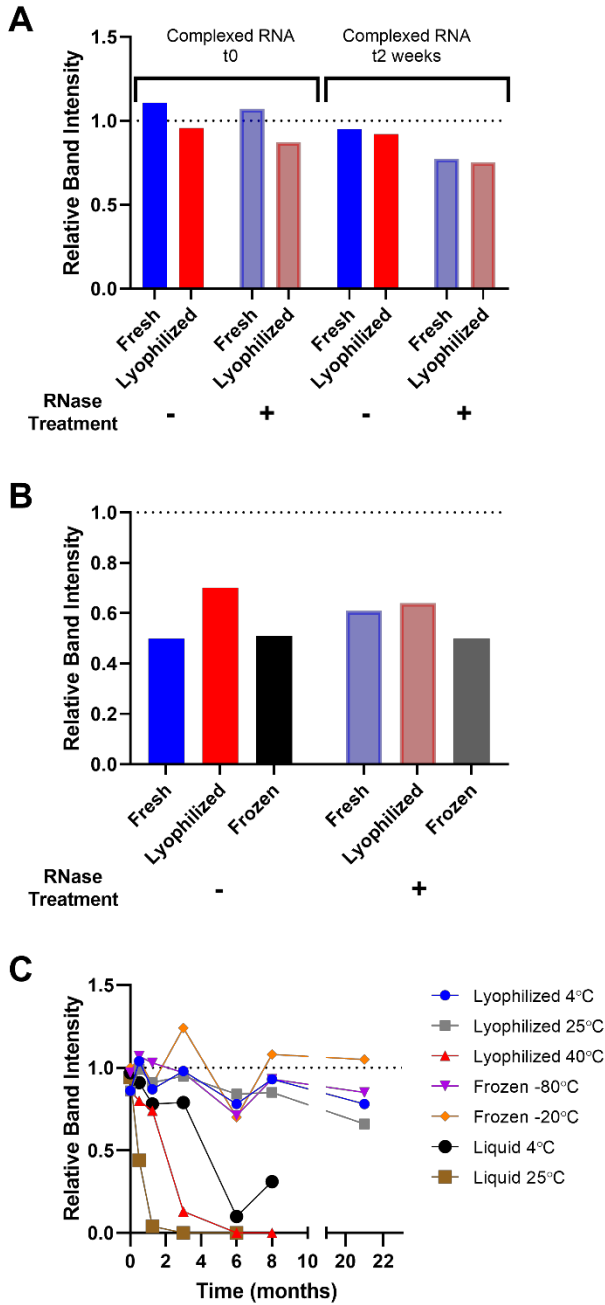


**Figure S5.**

Densitometry analysis of agarose gel images. (A) Quantitation of the main Zika saRNA band intensity for the agarose gel image in Figure 2A. The intensity of the RNA band extracted from fresh and lyophilized complexes before and after RNase treatment is quantified for each sample relative to the uncomplexed RNA loading control which was set to have an intensity of 1. (B) Quantitation of the main OVA mRNA band intensity for the agarose gel image in Figure 3A. The intensity of the RNA band extracted from fresh, lyophilized, and frozen complexes before and after RNase treatment is quantified for each sample relative to the uncomplexed RNA loading control which was set to have an intensity of 1. Note that in this gel image the uncomplexed RNA loading control band had a higher intensity than the bands for the complexed samples. Therefore, the relative band intensity for the complexed samples is roughly 50-60%

compared to the control but are comparable relative to each other. (C) Quantitation of the main SEAP saRNA band intensity for the Un-Treated agarose gel images in Figure 4C and Supplemental Figure S3. The intensity of the Un-Treated RNA band extracted from stored complexes is quantified for each sample relative to the freshly complexed positive control ("Fresh") prepared each analysis day which was set to have an intensity of 1.